Estimation of the shape error in the Long workpiece from the normal grinding force of cylindrical traverse grinding

Koichi Sakamoto[1,a *], Takashi Onishi[1,b], Moriaki Sakakura[2,d], Naoki Kawaguchi[3,c] and Kazuhito Ohashi [1,e]

[1]Graduate school of Okayama University,
3-1-1 Tsusima-naka, Kita-ku, Okayama, 700-8530, JAPAN

[2]Daido University,
10-3 Takiharucho, Minami-ku, Nagoya, 457-8530, JAPAN

[3]Graduate school of Daido University,
10-3 Takiharucho, Minami-ku, Nagoya, 457-8530, JAPAN

[a]p5ye8cgr@s.okayama-u.ac.jp, [b]onishi@mech.okayama-u.ac.jp,
[c]sakakura@daido-it.ac.jp, [d]dmm1703@stumail.daido-it.ac.jp, [e]k-ohashi@okayama-u.ac.jp,

Keywords: Cylindrical traverse grinding, Elastic deformation, Slender workpiece, Shape error, Normal grinding force

Abstract. In cylindrical traverse grinding of a slender workpiece, the elastic deformation of the workpiece is caused by the normal grinding force. Due to the low stiffness of a slender workpiece, the workpiece shape error tends to increase especially at the end edge where the wheel draws away from the workpiece. This shape error observed at the end edge of the workpiece has great influence on the shape accuracy of the ground workpiece. Therefore, it is necessary to reduce the shape error at the end edge to improve the shape accuracy. The purpose of this study is to estimate the shape error at the end edge of the workpiece to explore appropriate grinding conditions. The shape error of the ground workpiece was estimated by calculating the elastic deformation of the ground workpiece based on the measured normal grinding force. The estimated shape error agreed well with the measured one of the actually ground workpiece. Investigation compared the shape error of the ground workpiece with the estimated one from the normal grinding force measured during the process.

Introduction

The slender workpiece such as automobile axle parts and oil hydraulic cylinders is finished by cylindrical traverse grinding. The ground workpiece is bends under the normal grinding force during the process because of low stiffness as shown in Fig. 1(a). Fig. 1(b) shows the shape error of the slender workpiece caused by the elastic deformation during the grinding process. To reduce the shape error, a workpiece rest is generally used[1]. However, spark-out grinding is not good for efficiency and there are few scientific setting criteria to use rests

appropriately.

In this study, we found that the main cause of the shape error is the normal grinding force[2]. We have proposed an advanced grinding method to reduce the shape error of the workpiece by controlling the traverse speed during grinding[3].

In this report, we investigated the effect of changing the grinding conditions on the shape error. Some reference books suggest that the contact width when the grinding wheel start to interfere the workpiece should be two thirds of the wheel width[4]. Fig. 1(b) shows the most recommended contact width between the grinding wheel and the workpiece is two third of the grind wheel width. However no study is found to determine the contact width when the wheel is retracted at the end edge of the workpiece. In this study, we optimized the contact width of the grinding wheel at the end of the grinding process. Several grinding experiments were carried out by changing the contact width of the grinding wheel at the end of the process.

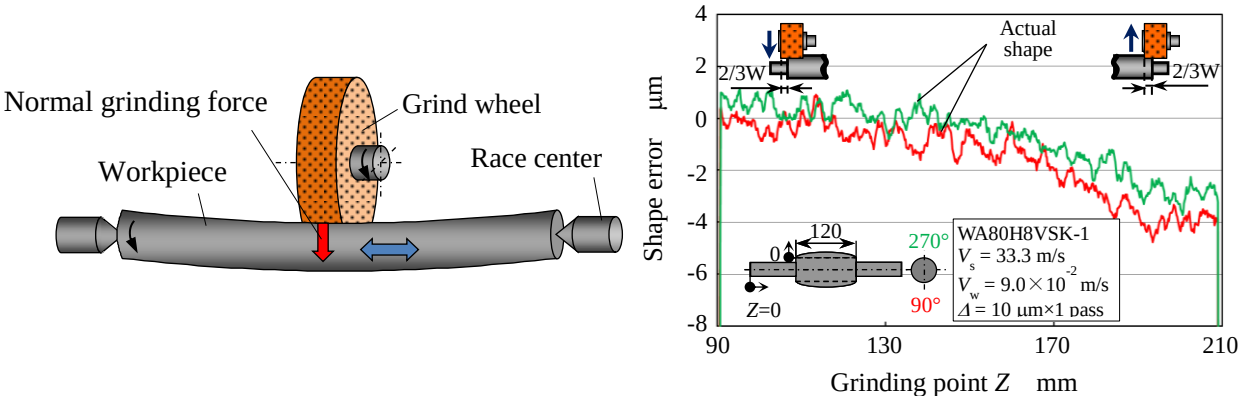

(a) Elastic deformation of a workpiece during grinding process

(b) Measured shape of the ground workpiece

Fig. 1 The shape error of a workpiece caused by the elastic deformation in grinding process

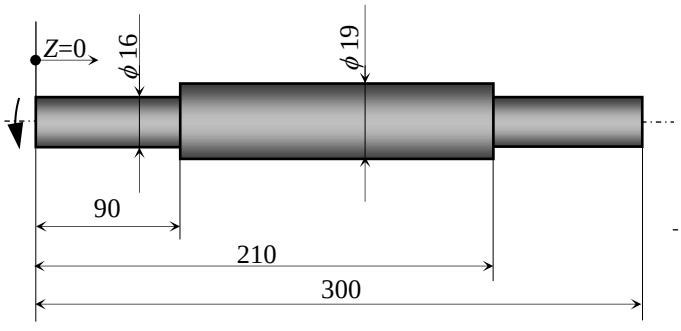

Fig. 2 Slender workpiece

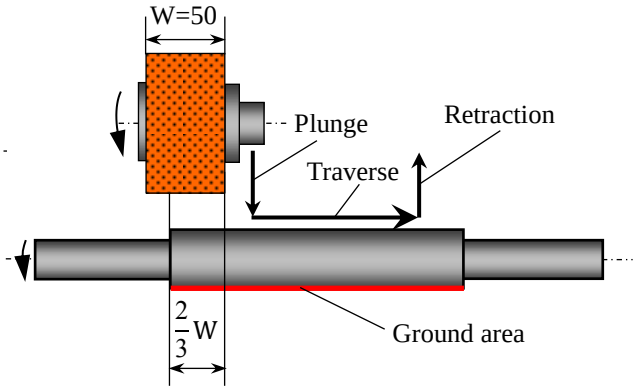

Fig. 3 Wheel motion of traverse grinding

Grinding conditions

Fig. 2 shows the slender workpiece used in this study. It's aspect ratio is over 15. The middle part of 19 mm in diameter is ground. Before grinding experiments the workpieces are finished in slender spark-out duration to minimize the shape error. Grinding forces were

measured by strain gauges mounted to the race centers[5].

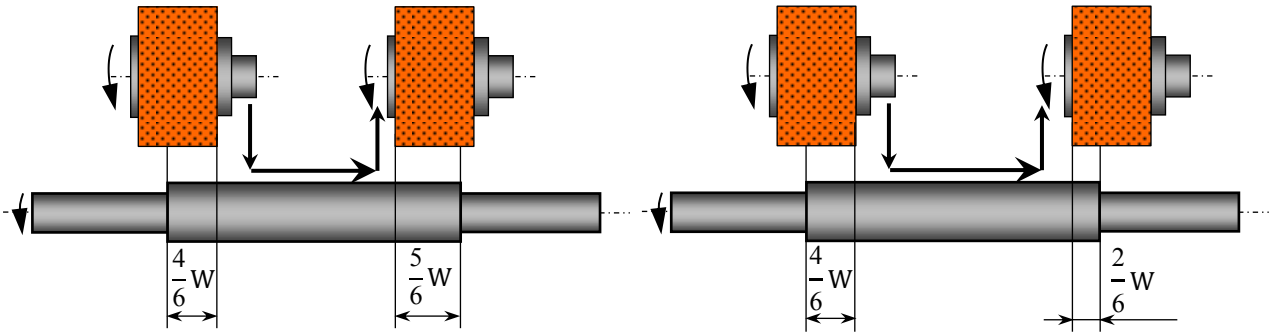

(a) Grinding conditon A (b) Grinding condition B

Fig. 4 Wheel motion in each grinding condition

In this study, the workpiece was ground under conditions shown in Fig. 4. At first, the wheel was fed to radial direction. The contact width of the grinding wheel at the beginning of the process was two thirds. After giving feed by 10 μm, the grinding wheel was started to traverse. The contact width when the wheel was retracted at the end edge of the workpiece was changed in two conditions as shown in Fig. 4 (a) and (b). Table 1 shows the main grinding conditions. The shape of the ground workpiece was measured with a laser displacement gauge by scanning in the axial direction.

Table 1 Main grinding conditions

Grinding machine	GE-4P CNC Grinding machine (JTEKT)
Grinding wheel	WA80H8VSK-1 ϕ380×W50 [mm]
Wheel contact width at plunge process	(A)33.3 [mm](4/6 of wheel width) (B)33.3 [mm](4/6 of wheel width)
Wheel contact width at wheel retraction	(A)41.7 [mm](5/6 of wheel width) (B)16.7 [mm](2/6 of wheel width)
Peripheral wheel speed	V_s = 33.3 [m/s]
Peripheral workpiece speed	$V_w = 9.0\times10^{-2}$ [m/s]
Depth of cut	Δ = 10 [μm]×1 [pass]
Traverse speed	V_f = 12.2 [mm/s]
Grinding fluid, Flow rate	Soluble type, 80 times dilution, Q =20 [ℓ/min]

Estimation method of the elastic deformation of the ground workpiece

The elastic deformation of the slender workpiece was calculated using the beam model which is suported at both ends and bended by the normal grinding force as shown in Fig. 5. In this model, the normal grinding force applied to the center of the ontact width between the wheel

and the workpiece. The elastic deformation of the workpiece was calculated from equation (1). C_1 and C_2 were integral constants. These were calculated from equation (2) and (3). Variables used in these equation were shown in Fig. 5. Yang's module E was 206 GPa because the groung material was carbon steel C45. The elastic deformation δ of the ground area was obtained by calcualating the equation (1) with changing the Z_g, which is the axial positional coordinate of loading point, between L_1 and L_2 in Fig. 5.

$$\delta=\frac{P}{EI_2}\left\{\frac{1}{6}\left(\frac{Z_g}{L_3}-1\right)Z^3+C_1Z+C_2\right\} \tag{1}$$

$$C_1=\frac{Z_gL_3I_2}{3I_3}-\frac{1}{2}Z_g^2-\frac{1}{6L_3}\left\{2\left(\frac{I_2}{I_1}-1\right)\left(1-\frac{Z_g}{L_3}\right)L_1^3-Z_g^3\right\}+Z_gL_2\left(1-\frac{I_2}{I_3}\right)\left(\frac{1}{3}\frac{L_2^2}{L_3^2}-\frac{L_2}{L_3}+1\right) \tag{2}$$

$$C_2=\frac{1}{3}\left(\frac{I_2}{I_1}-1\right)\left(1-\frac{Z_g}{L_3}\right)L_1^3 \tag{3}$$

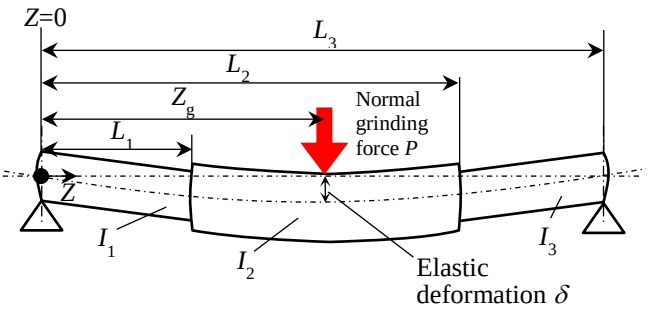

Fig. 5 Calculation model of elastic deformation

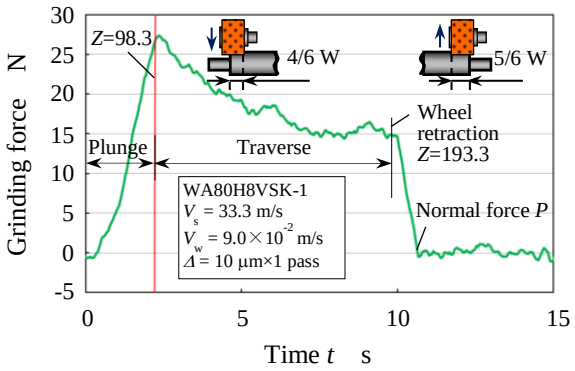

Fig. 6 Variation of grinding force

Fig. 6 shows the measured normal grinding force P obtained by the grinding test performed in the grinding conditon A in Table 1. In this graph, the wheel was started to traverse at the red line. Fig. 7 shows calculated results of elastic deformation of the workpiece as the grinding point was moved to the middle part of the workpiece. From these results, initially the grinding point existed between 25 to 28 mm, which is from the end of the grinding part (Z_g=115 to 118 mm), the elastic deformation of the workpiece decreased rapidly as the grinding point moved to the middle part of the workpiece. However the elastic deformation of the workpiece was not changed slightly when the middle part of the grinding area was reached to 29 mm (Z_g=119 mm). Between Z_g=115 to 118 mm the shape was the elastic deformation at the rear end edge of the grinding wheel was preserved as the ground surface because the elastic deformation had the maximum value. When Z_g=119 mm, the elastic deformation was transferred to the workpiece surface between Z=94 to 119 mm. In this study, the shape was estimated under the assumption that the elastic deformation at the central point of grinding area was transferred as slender as the normal grinding force was not changed significantly. Therefore the shape error between Z_g=119 to 189.2 mm was estimated

by calculating the elastic deformation at the loading point where was the central area of the grinding area. When Z_g=189.2 mm, the traverse motion stopped and the grinding wheel was retracted. Therefore the elastic deformation at the moment of the wheel retraction was preserved to the workpiece surface between Z=189.2 to 210 mm. Using this method, the estimated shape error is shown in Fig. 8.

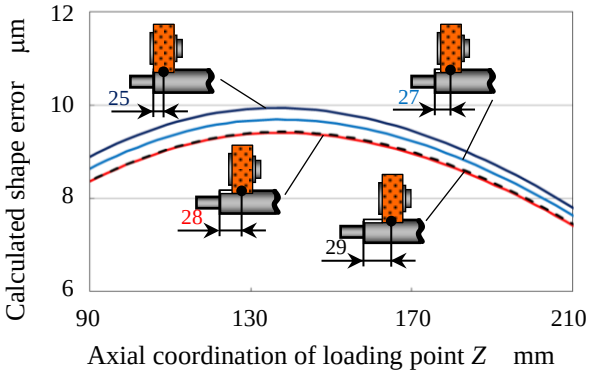

Fig. 7 Estimation of Elastic deformation for each grinding point

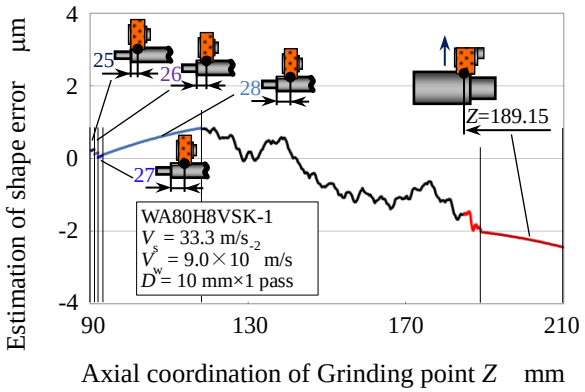

Fig. 8 Estimated shape error of ground workpiece

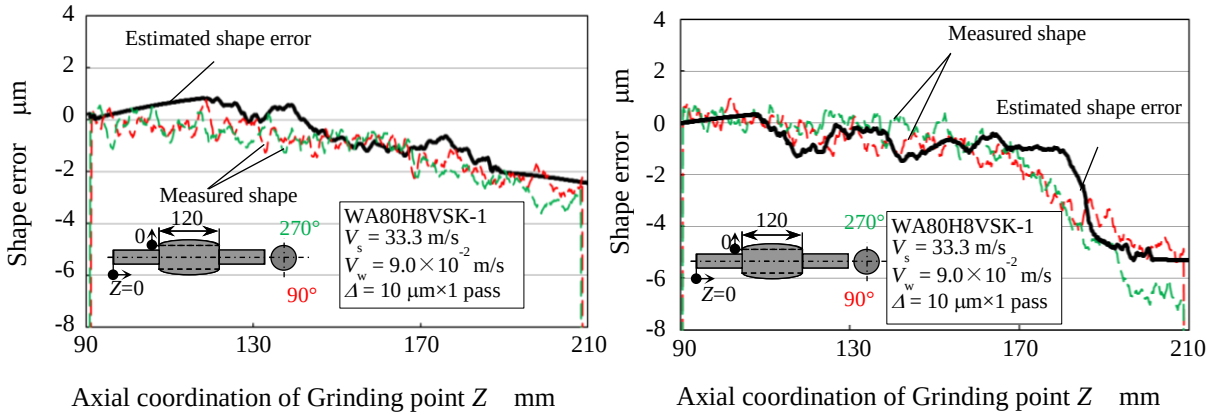

(a) Condition A (b) Condition B

Fig. 9 Measured grinding force in each condition

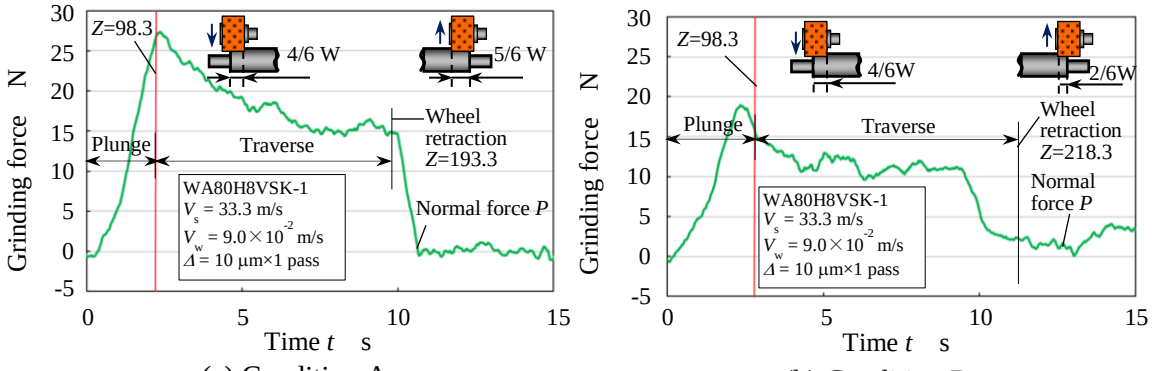

(a) Condition A (b) Condition B

Fig. 10 Measured shape of workpiece and estimated shape error in each condition

Comparison of measured results of shape error in two grinding conditions

Fig. 9 shows the results of measured normal grinding force. Fig. 10 shows the shape of ground workpiece and the calculated shape error of the workpiece. In Fig. 10, measured shape and estimated one were agreed well. Compared Fig. 9 (a) with (b), the normal grinding force was decreased before the grinding wheel retracted in the condition B. To reduce the shape error, it is important to prevent the rapid change of normal grinding force before the wheel retraction.

Conclusions

In this study, to reduce the shape error of the workpiece during the cylindrical traverse process of a slender workpiece, the shape error of the workpiece was estimated from elastic deformation of the workpiece. Main conclusions obtained in this study as follows;

(1) The elastic deformation of workpiece calculated from normal grinding force agreed well with the measured shape of ground workpiece.

(2) It was conformed that the rapid change of normal grinding force causes the shape error of the workpiece.

References

[1] K. Kounosu, Characteristics of Pneumatic Workrest –A Case of One Pass Traverse Grinding-, J. of JSPE, 56 (1990) 147-152.

[2] T. Takashima, T. Onishi, M. Sakakura, K. Ohashi and S. Tsukamoto, Improvement in the Shape Error of the Long Workpiece in Cylindrical Traverse Grinding, The 19th International Symposium on Advances in Abrasive Technology, Stockholm, Sweaden, (2016) 3-5.

[3] T. Onishi, T. Kodani, K. Ohashi, M. Sakakura, and S. Tsukamoto, Study on the Shape Error in the Cylindrical Traverse Grinding of a Workpiece with High Aspect Ratio, Advanced Materials Research, 1017 (2014) 78-81.

[4] K. Ai, Grinding one point lesson, J. of JSAT, 52 (2008) pp. 42(in Japanese).

[5] S. Tsukamoto, T. Ohashi, T. Fujiwara, Measurement Technology for Grinding, Yokendo, Tokyo, 2005, pp. 33(in Japanese).